

Vibrational microspectroscopy of food. Raman vs. FT-IR

Lisbeth G. Thygesen,
Mette Marie Løkke[†],
Elisabeth Micklander and
Søren B. Engelsen*

Centre for Advanced Food Studies, Department of
Dairy and Food Science, The Royal Veterinary and
Agricultural University, Rolighedsvej 30, DK-1958
Frederiksberg C, Denmark (tel: +45-35-2832-05;
fax: +45-35-2832-45; e-mail: se@kvl.dk)

FT-IR and Raman spectroscopy are complementary techniques for the study of molecular vibrations and structure. The combination with a microscope results in an analytical method that allows spatially resolved investigation of the chemical composition of heterogeneous foods and food ingredients. The high spatial resolution makes it possible to study areas down to approximately $10 \times 10 \mu\text{m}$ with FT-IR microspectroscopy and approximately $1 \times 1 \mu\text{m}$ with Raman microspectroscopy. This presentation highlights the advantages and disadvantages of the two microspectroscopic techniques when applied to different heterogeneous food systems. FT-IR and Raman microspectroscopy were applied to a number of different problems related to food analysis: (1) *in situ* determination of starch and pectin in the potato cell, (2) *in situ* determination of the distribution of amygdalin in bitter almonds, (3) the composition of blisters found on the surface of bread, (4) the microstructure of high-lysine barley and (5) the composition of white spots in the shell of frozen shrimps.

© 2003 Elsevier Science Ltd. All rights reserved.

* Corresponding author.

[†] Present affiliation: Arla Foods amba.

Introduction

Infrared (IR) and Raman spectroscopy are complementary techniques that provide information on molecular structure. By combining spectroscopy with microscopy molecular information can be obtained with great spatial resolution at the microscopic level. Samples of microscopic size can be analysed directly, in air, at ambient temperature and pressure, wet or dry, and in many cases without destroying the sample.

Both qualitative and quantitative information can be obtained using microspectroscopy. A number of organic compounds and functional groups can be identified by their unique pattern of absorption, and the intensity of the absorption may be used for the calculation of the relative concentration in the sampled entity (Wetzel & LeVine, 1999).

FT-IR and Raman microspectroscopy may be combined with at least three different mapping techniques: point, line and area. With point acquisition several spectra are measured from different places in a sample selected after visual inspection through the microscope, i.e. the spectra are not systematically related to each other spatially. Line mapping defines a series of spectra to be obtained along one dimension (a line) and can be used to investigate changes in a chemical component along a certain direction, i.e. a profile. An area map uses two dimensions, providing a spectroscopic image that can be directly compared to the corresponding visual image, but with an entire spectrum in each pixel instead of a simple colour. By using a series of partly overlapping acquisition areas it is possible to obtain a smoothing of a profile or a map. Using a standard microscope equipped with an XY stage it may take up to several hours to map a few square millimetres, even for an FT-based instrument. However, new instruments that record an entire row (i.e. a line scan) simultaneously by use of a CCD array will make area mapping much less time consuming.

Vibrational microspectroscopy offers many possibilities for the study of biological material, including foods systems. In this presentation we demonstrate the potential of the method by relaying examples from our laboratory where IR or Raman microspectroscopy has been successfully applied to potatoes, bitter almonds, bread, barley kernels and shrimp shells to obtain information about microstructure and chemical composition.

Raman or infrared microspectroscopy for food studies

Both Raman and infrared microspectroscopy may reveal useful information about food samples. In infrared spectroscopy the sample is radiated with infrared light. Different chemical bonds absorb at different infrared wavelengths depending on the atoms connected, the surrounding molecules, and the type of vibration the absorbance gives rise to (for example stretching or bending). In Raman spectroscopy, the sample is radiated with monochromatic visible or near infrared light from a laser. This brings the vibrational energy levels in the molecule to a short-lived, high-energy collision state, which returns to a lower energy state by emission of a photon. Normally the photon has a lower frequency than the laser light (Stokes Raman scattering), and the difference in frequency (given in reciprocal centimetres) between the frequency of the laser and that of the scattered photon is called the Raman shift. The Raman shift corresponds to the frequency of the fundamental IR absorbance band of the bond.

Even though both methods probe molecular vibrations and structure, they do not provide exactly the same information. While IR spectroscopy detects vibrations during which the electrical dipole moment changes, Raman spectroscopy is based on the detection of vibrations during which the electrical polarisability changes (Pistorius, 1995). As a rule of thumb, this implies that bonds that connect two identical (or nearly identical) parts of a molecule tend to be more active in Raman than in IR spectroscopy. For example, the C=C bond is generally more intense in Raman than in IR spectra. Characteristic absorbance bands found in food systems are shown in Table 1 for both IR and Raman. The table shows that all four major food ingredients (water, fat, protein and carbohydrates) absorb both in Raman and IR, but that the intensities of the absorbance bands vary. An important difference to note is that the O–H stretching vibration is very strong in IR, but very weak in Raman, because OH bonds are only weakly polarisable. For this reason, water is practically “invisible” in Raman spectroscopy, while it dominates the IR spectrum, if present. The other three major ingredients are visible with both types of spectroscopy, albeit their Raman and IR spectra are not identical, because the relative intensities differ for the bands making up the spectrum of each ingredient. Unless a sample has too high a water content to be effectively studied using IR, other factors will determine which of the two types of spectroscopy best solves a given problem. Table 2 lists characteristics of the two techniques that are important to consider when analysing food samples. Raman spectroscopy has the potential of a better spatial resolution due to the lower wavelengths used, and furthermore offers confocality, i.e. it is

possible to focus on different planes below the sample surface. It is, for example, possible to focus beneath a quartz plate or through a food packaging material to obtain pure spectra of food samples without exposing the food to the atmosphere. On the other hand, the signal-to-noise ratio is much lower, and if the sample fluoresces, measurements may even be impossible. For example, measurements on samples that contain one or more of the three fluorescent amino acids (tyrosine, tryptophan and phenylalanine) or chlorophyll may prove difficult or, in practice, impossible to study by Raman spectroscopy. However, the problem may be overcome if a Raman instrument is equipped with a near infrared laser instead of a laser in the visible range, though the spatial resolution would be poorer. Another problem related to Raman spectroscopy is heating of the sample (West, 1996). The heat generated by the laser may alter or even destroy the sample during measurement. In some cases, the best setting of the Raman instrument is therefore a compromise between destructive heating, which calls for short sampling times, and a high signal to noise ratio, which calls for long sampling times and/or repeated samplings.

The characteristics of IR and Raman spectroscopy mentioned in Table 2 and discussed above apply both to normal macroscopic IR and Raman spectroscopy and to microspectroscopy. In macroscopic IR or Raman spectroscopy the combination of small sampling areas and heterogeneous food samples is often a problem, because it calls for homogenisation of the samples prior to spectral analysis or for repeated sampling of each sample in order to obtain representative spectra. However, with microspectroscopy this combination is turned into an advantage, because it offers the possibility of studying the food heterogeneity in detail, the only concern being that the heterogeneities to be studied must be on a larger scale than the spatial resolution obtainable with the instrument used. In other words, it must be possible to find homogeneous areas in the sample that are larger than or equal to the smallest possible acquisition area, if characteristic spectra of the feature(s) are to be obtained. In the food industry, microspectroscopy is thus most often called for in situations where the objective is identification of advantageous or disadvantageous microscopic features of food samples. For this reason microspectroscopy remains a laboratory technique for experts, while on-line solutions for quantitative spectroscopy are out of the question, at least with the present technology.

Food applications

In situ starch and pectin in the potato cell

FT-IR microscopy has previously been utilised to characterize pectins in the cell wall of plants (McCann *et al.*, 1997). In this study Raman microspectroscopy was used to measure pectin in raw potato tubers,

Table 1. Infrared and Raman characteristic group frequencies (Naumann et al., 1991; Pistorius, 1995 and Piot et al., 2000)

Frequency, cm ⁻¹		Group Vibration	Intensity [#]		Description	Mainly observed in
4000	3000		IR	Raman		
		O-H stretch	vs	vw	Hydroxyl	Liquid phase
		=C-H stretch	s-m	m	Unsaturated	Lipids
		-C-H stretch	s-m	m	Saturated	Lipids
		-C≡N stretch	m	s	Nitrile	
		C=O stretch	s	m-w	Ester	Lipids, Amino Acid
		C=O stretch	s	w-m	Carboxylic acid	Lipids, Amino Acid
		C=O stretch	s	m-s	Amide I	Proteins
		C=C stretch	m-w	s	Not conjugated	Lipids
		C=C stretch	m	s	<i>Trans</i>	Lipids
		C=C stretch	m	s	<i>Cis</i>	Lipids
		N-H bending	s	w	Amide II	Proteins
		C-H scissoring	m	m-w	Aliphatic -CH ₂	Lipids
		C-O stretch	s		Carboxylates	Amino Acids, Lipids
		N-H bending	w-m	var	Amide III	Proteins
		P=O stretch	vs	m-w	Phosphate ester	Lipids, Nucleic Acids
Fingerprint from skeleton						
		C-O stretch	s	m-w	Ether	Carbohydrates
		Skeletal mode		m	α-(1→4) linkage	Starch
		C-O-C skeletal	m-w	m-w	β-configuration	Glucose, galactose, mannose
		C-O-C skeletal	m-w	m	α-configuration	
		C-H rocking	w-m	vw	Aliphatic -CH ₂	Lipids
		Skeletal mode		vs		Starch

[#] s = strong, m = medium, vs = very strong, vw = very weak

generating spectra directly from the “intact” potato cell wall. In the cell wall, pectin shows a unique galacturonic methyl ester peak in the area around 1745 cm⁻¹, where the surrounding and dominating starch granules in the cell do not have signals that interfere (Figure 1).

Using the Raman microscope, it proved difficult to locate the pectin signals and obtain good signals before the open cell wall collapsed, which it did after a few minutes. Characteristic starch spectra were easily recorded by focusing on the individual starch granules in the cell. The pectin spectrum in Figure 1 indicates the presence of some fluorescence emission, but in this case an efficient green laser (532 nm) could be used to measure the potato cells, even though the green light gave rise to fluorescence.

Results. It was found to be ideal to cover the sample with a quartz cover slip to maintain the integrity of the cell wall. The pectin spectrum in Figure 1 is the best pectin spectrum recorded directly from the cell wall through a cover slip with a long-working-distance objective (2.4 mm). The strong Raman band at 474 cm⁻¹ in a pectin and/or starch spectrum indicates that starch is measured, and not the pectin. Pectin was characterised by signals near 858 cm⁻¹ (α-anomer carbohydrate and indicative of a very low degree of esterification), at 1455 cm⁻¹ (ester O-CH₃ stretch) and at 1745 cm⁻¹ (ester carbonyl C=O stretch). The signal near 1000 cm⁻¹

indicates that aromatic compounds interfere with the pectin spectrum. The starch spectrum in Figure 1 is of remarkable quality, equal to or even better than a typical Raman spectrum obtained from isolated and purified potato starch. This indicates that the high crystallinity of the intact granule is well reflected in the spectrum.

Conclusions. It was possible to measure high-quality starch and pectin spectra directly in the potato cell wall with Raman microscopy using a green 532 nm laser. However, it remains to be elucidated whether the Raman spectra are sufficiently distinct to be able to distinguish between different qualities of the two substances in different potato cultivars and/or in different transgenic potatoes.

The distribution of amygdalin in bitter almonds

Cyanogenic glycosides contain a nitrile group (-C≡N), and upon hydrolysis they liberate the toxic compound hydrogen cyanide (HCN). Due to the relatively rigid triple bond, the nitrile group has special vibrational characteristics. Cyanogenic glycosides are accumulated in a number of plants as a defence system against fungi and pests. Bitter almonds contain the cyanogenic glycoside amygdalin.

Micklander, Brimer, and Engelsen (2002) developed a method for assessment of the content and distribution of amygdalin in bitter almonds. A part of their study

Table 2. Raman spectroscopy vs. Infrared (IR) spectroscopy

	IR spectroscopy	Raman spectroscopy
Water	Strong	Very weak
Spatial resolution	$\geq 10 \mu\text{m}^2$	$\geq 1 \mu\text{m}^2$
Signal-to-noise	High	Low
Fluorescence	None	Can be devastating
Heat induction	Negligible	Strong
Confocality	No	Yes

concerned *in situ* determination of the distribution of amygdalin across the cotyledon within a bitter almond. Raman microspectroscopy was chosen, because nitrile groups ($-\text{C}\equiv\text{N}$) give rise to relatively low intensity bands in IR spectroscopy (very small changes in dipole moment), whereas they are strongly Raman active (large change in polarisability during stretching vibrations), see Table 1. The nitrile vibration band is highly specific, as the nitrile group is rarely found in natural compounds. The band is found near 2240 cm^{-1} in the Raman spectrum (Figure 1) and this area is almost free from interference from other chemical components (Table 1). The aromatic ring found in amygdalin is also strongly Raman active, but the specificity is low, because aromatic compounds are ubiquitous in nature.

Results. Figure 2 shows the content of amygdalin across the cotyledon for every $33.3 \mu\text{m}$ along a straight line of the transversely sectioned slice of two different bitter almonds. The content is expressed as the area of the nitrile peak in the Raman spectrum. The figure shows that amygdalin was not present in measurable amounts in the centre of the two almonds, but that small quantities were found 0.5 mm from the centre. The content generally increased towards the epidermis, but with large local fluctuations (up to 500% within $33.3 \mu\text{m}$). As amygdalin functions as a defence against attacking insects or fungi, high concentrations near the surface of the almond make sense.

Conclusions. Raman microspectroscopy proved to be a rapid and non-destructive method for probing the distribution of amygdalin in bitter almond cotyledons. The advantages of using the nitrile vibration band are that the band is located in a spectral range with no interference from other chemical compounds and that the nitrile group is specific for amygdalin, when studying bitter almonds.

The composition of blisters found on the surface of bread

When dough is stored at low temperatures prior to baking, a phenomenon called blistering can arise on the crust of the bread. Blisters are small white bulges on the crust of the bread with a diameter of $0.5\text{--}5 \text{ mm}$. One theory is that oil particles rise to the surface of the bread, creating an increased concentration of lipids. The composition of the blisters and especially the content of starch

and gluten were studied and compared with the content of these components in the breadcrumb and crust.

IR microspectroscopy was chosen for this study, as fluorescence from maillard compounds in the crust and from certain amino acids made Raman spectroscopy impossible, at least when using a laser in the visible range. With the microscope it was possible to focus on different locations on the inside of blisters and to obtain good quality spectra from these positions.

Results. The characteristic vibrational bands of pure gluten and starch were found using FT-IR microspectroscopy in reflectance mode. It was found that the bands in the ranges $1663\text{--}1630$ and $1595\text{--}1528 \text{ cm}^{-1}$ could differentiate between spectra of blisters and of breadcrumb from comparable positions just below the crust. The two wavelength ranges are characteristic of the amide I band (overlapped with the HOH bending vibration from water) and the amide II band from gluten (Table 1). The spectra of the inside "walls" of the blisters showed higher intensity at the "starch" band and lower intensity at the "gluten" band compared to breadcrumb. This strongly indicates that the ratio of starch to gluten was higher in the breadcrumb just around the blisters than in the ordinary breadcrumb.

Conclusions. The observation that the gluten content is lower in the blister walls than in breadcrumb could explain why blisters are developed. The blisters may be developed in spots on the surface of the bread where the gluten network in the dough/breadcrumb below the developing crust is too weak to withhold the CO_2 produced by the yeast during the baking process. The CO_2 is then instead trapped in the crust, causing blisters. One can speculate that such areas develop because of condensation of water on the surface of the cold dough in the beginning of the baking process. In contrast to the gluten network, small starch grains could diffuse into wetted parts of the surface and part of the surface would therefore become rich in starch. In any case, FT-IR microspectroscopy made it possible to study the microstructure inside blisters, and the technique provided new information about this yet unsolved problem.

The microstructure of high-lysine barley

The nutritional value of barley is limited by a low content of essential amino acids. The primary limitation is lysine, and the nutritional value of barley can be improved significantly by increasing the lysine content (Munck, Karlsson, Hagberg, & Eggum, 1970; Newman & McGuire, 1985; Shewry, Williamson, & Kreis, 1987; Munck, 1992). Albumins and globulins contain high concentrations of lysine and exist primarily in the embryo and the aleurone layer. Since the storage proteins, prolamines and glutelins exist in the endosperm, a larger embryo and a thicker aleurone layer would result in higher concentrations of essential amino acids in barley.

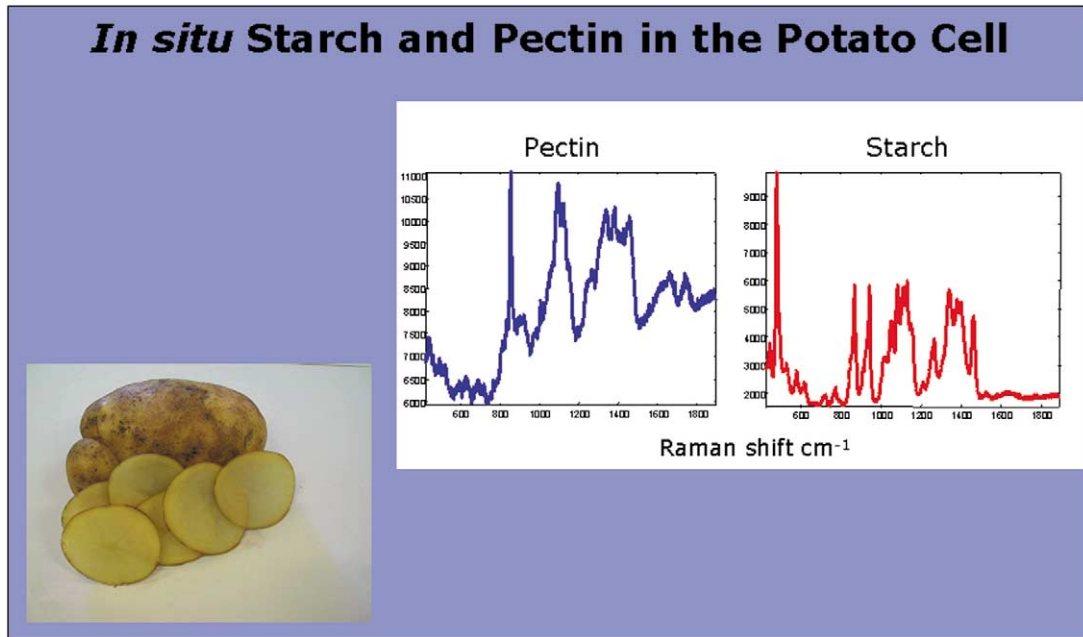


Fig. 1. Raman spectra of pectin and starch obtained directly in the potato cell using a LabRam Infinity instrument equipped with a green laser (532 nm, Nd:YAG), a Peltier-cooled CCD detector and a long working distance 100× Leica objective. Laser power at the sample was approximately 40 mW.

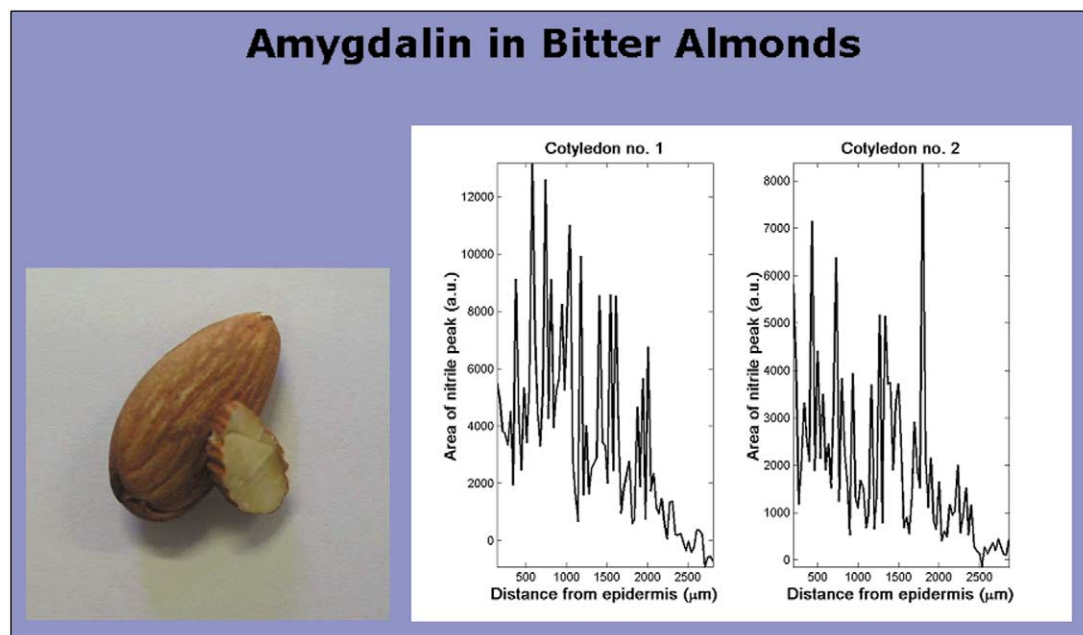


Fig. 2. Raman measurements of amygdalin in bitter almond cotyledons using the same equipment as in Fig. 1. The plots show for two different almonds the area of the nitrile peak at approximately 2242 cm^{-1} for 81 positions along a line from the epidermis to the centre of the almond.

Barley kernels can be forced to mutate by inhibiting the synthesis of prolamines and thereby increase the lysine content of barley. The mutant, *Riso 1508*, and its mother sort, *Bomi*, were investigated here with FT-IR microspectroscopy in order to describe the microstructure of the barley kernels. In addition to the difference in lysine content, it is well known that the *Riso*

1508 mutant has lower starch content than *Bomi*. It is well-known that the two cultivars differ with regard to the protein composition and with regard to the ratio between protein-N and amide-N. The amide-N content is approximately 16% of the protein-N content in case of *Riso 1508*, while it is approximately 12% for normal barley (Munck *et al.*, 2001). In a comprehensive study

by Piot, Autran, and Manfait (2000) the content of protein in wheat kernels was measured using Raman microspectroscopy that offers higher spatial resolution.

For measurements in transmittance, slices of kernels had to be 4 μm or less in order to keep the absorbance within an acceptable limit. After slicing of the kernels it was necessary to keep the slices between two cover slips to avoid curling. During measurement the cover slips were removed, and the slice was placed on a ZnSe plate. Area scans were used to map the contents and distribution of macromolecules in the slices. A smoothing of the obtained maps was obtained by making the distance between neighbour acquisitions equal to half the length of the side of the square acquisition area. The area scan generated from a slice of *Risø 1508* consisted of 25×38 scans and of 34×44 scans from a slice of *Bomi* (Figure 3).

Results. Specific wave numbers were chosen to indicate the contents of different macromolecules, i.e. 1543 cm^{-1} (Amide II) was chosen to indicate protein, 1148 cm^{-1} (coupled C–C and C–O vibrations) to indicate carbohydrate, and 1738 cm^{-1} (C=O stretch) to indicate the content of lipid. The ratio between 3100 cm^{-1} (primary amide) and 3300 cm^{-1} (primary amide + secondary amide) was used as an indication of the amount of amide-N and protein-N, respectively.

It was found that protein primarily exists in the borderline of the kernel, but no difference was found between the content of protein between *Risø 1508* and *Bomi*. However, an indication of relatively higher amide-N content in *Risø 1508* than in *Bomi* was found

(Figure 3, Left). In *Bomi*, carbohydrates were concentrated in a specific area, whereas in *Risø 1508* they were found over most of the border (Figure 3, Right). The characteristic band of lipids ($\sim 1738\text{ cm}^{-1}$) did not show any specific variations.

Conclusion. With IR microspectroscopy it was possible to obtain an indication of the composition and distribution of the macromolecules in the two cultivars of barley and the difference between them was evident, especially the spatial distribution of carbohydrate differed between the two cultivars. The results are, however, only indicative as the required thinness of the slices ($\sim 4\text{ }\mu\text{m}$) made it difficult to make slices with approximately the same thickness, which created problems with higher absorbance from thicker slices.

The composition of white spots developing in shrimp shells during frozen storage

Raw shrimps are a valuable food, and they are furthermore used for food decoration in Asian countries. Consequently, the appearance of the shrimps is an important quality parameter. When shrimps of the species *Pandalus borealis* (pink shrimp) are still alive their shell appear transparent, but white spots may develop in the shell during transport, during which the shrimps are frozen. Mikkelsen *et al.* (1997) and Mikkelsen *et al.* (1999) used a number of techniques to identify the substances present in the white spots, among them FT-IR microspectroscopy, Raman spectroscopy, X-ray diffraction, differential scanning calorimetry and electron microscopy.

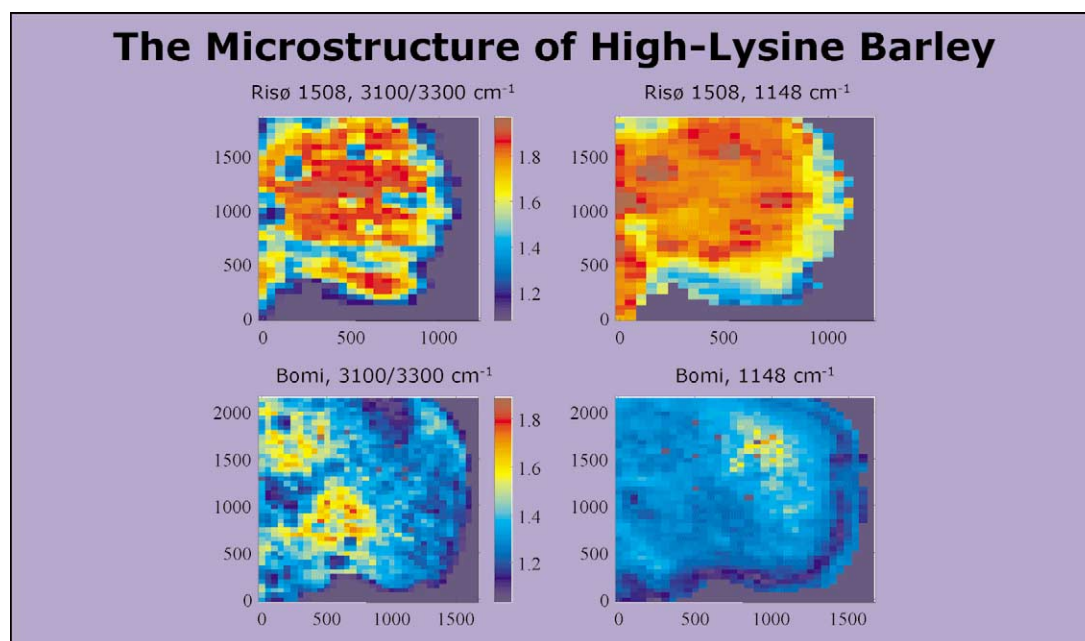


Fig. 3. Microstructure of barley as viewed by a FT-IR microscope. The area scans to the left are coloured according to the intensity ratio between 3100 cm^{-1} and 3300 cm^{-1} to indicate the amount of secondary amides, while the area scans to the right are coloured according to the intensity at 1148 cm^{-1} related to carbohydrate content. The instrument used was a Perkin Elmer System 2000 combined with an Autolmage microscope. The detector was a MCT detector (Mercury Cadmium Telluride, $10,000\text{--}700\text{ cm}^{-1}$) cooled with liquid nitrogen.

Results. By studying the IR and Raman spectra of the white spot areas and by comparing them to spectra of pure α -chitin and of a number of calcium carbonate polymorphs, it was found that the white spots consisted of amorphous α -chitin and $\text{CaCO}_3 \cdot 6\text{H}_2\text{O}$, known as ikaite, from the fjord in Greenland where this inorganic salt was first discovered. Ikaite degrades when brought to room temperature and instead the anhydrous calcium carbonates calcite and vaterite are formed.

Conclusions. The substances present in the white spots in shrimp shells were successfully identified. FT-IR microspectroscopy could not have solved the problem alone, but the technique gave a valuable contribution. Raman spectroscopy proved to be an exceptional good probe for monitoring the conversion of CaCO_3 hexahydrate to its anhydrous polymorphs due to the insensitivity of Raman spectroscopy to water and the high sensitivity of the technique to different inorganic crystalline arrangements.

Conclusions

Both Raman and FT-IR microspectroscopy offer information on the molecular vibrations and structure of food samples. Raman has an advantage because of its ease of sampling, its higher resolution and the possibility for confocal measurements, but the lower signal to noise ratio, the risk of damaging the sample with the laser, and especially autofluorescence of the sample may hamper its applicability and provide an option for FT-IR microspectroscopy.

In each of the food applications described, new information about the microstructure of the food system was found by the use of microspectroscopy. In the potato cell wall it was possible, but difficult, to record a Raman spectrum of pectin; however, high-quality spectra of individual starch granules in the potato cell were readily acquired. Using Raman microspectroscopy, it was possible to study the distribution of amygdalin in bitter almond cotyledons. FT-IR microspectroscopy showed that blisters in bread crusts contained relatively small concentrations of gluten and large concentrations of starch compared to the ordinary breadcrumb. FT-IR microspectroscopy also showed differences in the distribution of macromolecules between a barley mutant and its mother sort, and it helped identify white spots in shrimp shells as α -chitin and ikaite.

The success of microspectroscopy for such diverse applications as those outlined above shows the vast potential of this technique. Furthermore, future and ongoing development within the field of vibrational microspectroscopy, such as CCD-based imaging systems and NIR microscopy techniques, will no doubt extend the range of possible applications. NIR microspectroscopy may offer the ideal compromise between IR and Raman techniques, as it has the spatial resolution of Raman and the signal-to-noise ratio of IR.

Moreover, it is possible to measure through a quartz window, which is a great advantage in many situations. The holographic information carried by NIR spectra (convoluted combinations and overtones) has already proven its worth in numerous macroscopic applications in the food industry, and we believe that microspectroscopy will benefit from it as well.

Acknowledgements

The authors wish to thank the Centre for Advanced Food Studies and the Danish Agricultural and Veterinary Research Council for financial support. Robert Kold Hansen and fellow scientists at Danisco Cultor Denmark (Brabrand) are most gratefully acknowledged for valuable discussions and sample materials. Gilda Kischinovsky is acknowledged for assistance with the manuscript.

References

- McCann, M. C., Chen, L., Roberts, K., Kemsley, E. K., Sene, C., Carpita, N. C., Stacey, N. J., & Wilson, R. H. (1997). Infrared microspectroscopy: sampling heterogeneity in plant cell wall composition and architecture. *Physiologia Plantarum*, *100*, 729–738.
- Micklander, E., Brimer, L., & Engelsen, S. B. (2002). Non-invasive assay for cyanogenic constituents in plants by Raman spectroscopy: content and distribution of amygdalin in bitter almond (*Prunus amygdalus*). *Applied Spectroscopy*, *56*, 1139–1146.
- Mikkelsen, A., Andersen, A. B., Engelsen, S. B., Hansen, H. C. B., Larsen, O., & Skibsted, L. H. (1999). Presence and dehydration of ikaite, calcium carbonate hexahydrate, in frozen shrimp shell. *Journal of Agricultural and Food Chemistry*, *47*, 911–917.
- Mikkelsen, A., Engelsen, S. B., Hansen, H. C. B., Larsen, O., & Skibsted, L. H. (1997). Calcium carbonate crystallization in the α -chitin matrix of the shell of pink shrimp, *Pandalus borealis*, during frozen storage. *Journal of Crystal Growth*, *177*, 125–134.
- Munck, L., Karlsson, K. E., Hagberg, A., & Eggum, B. O. (1970). Gene for improved nutritional value in barley seed protein. *Science*, *168*(3934), 985–987.
- Munck, L. (1992). The case of high-lysine barley breeding. In P. R. Shewry (Ed.), *Barley, genetics, biochemistry, molecular biology and biotechnology* (pp. 573–602). Wallingford, Oxon: CBA International.
- Munck, L., Pram Nielsen, J., Møller, B., Jacobsen, S., Søndergaard, I., Engelsen, S. B., Nørgaard, L., & Bro, R. (2001). Exploring the phenotypic expression of a regulatory proteome-altering gene by spectroscopy and chemometrics. *Analytica Chimica Acta*, *446*, 171–186.
- Naumann, D., Helm, D., Labischinski, H., & Giesbrecht, P. (1991). The characterization of microorganisms by Fourier-transform infrared spectroscopy (FT-IR). Chapter 3. In W. H. Nelson (Ed.), *Modern techniques for rapid microbiological analysis* (1st ed.). New York: USA:VCH.
- Newman, C. W., & McGuire, C. F. (1985). Nutritional quality of barley. In D. C. Rasmusson (Ed.), *Barley* (pp. 403–456). Madison, WI: American Society of Agronomy.
- Piot, O., Autran, J. C., & Manfait, M. (2000). Spatial distribution of protein and phenolic constituents in wheat grain as probed by confocal Raman microspectroscopy. *Journal of Cereal Science*, *32*, 57–71.
- Pistorius, A. M. A. (1995). Biochemical applications of FT-IR spectroscopy. *Spectroscopy Europe*, *7*, 8–15.
- Shewry, P. R., Williamson, M. S., & Kreis, M. (1987). Effect of mutant

genes on the synthesis of storage components in developing barley endosperms. In H. Thomas, & D. Grierson (Eds.), *Developmental mutants in higher plants* (pp. 95–118). Cambridge, UK: Press syndicate of the University of Cambridge.

West, Y. D. (1996). Study of sample heating effects arising during

laser raman spectroscopy. *The Internet Journal of Vibrational Spectroscopy*, 1, 5.

Wetzel, D. L., & LeVine, S. M. (1999). Microspectroscopy — imaging molecular chemistry with infrared microscopy. *Science*, 285, 1224–1225.

AUTHORS

**If you want to make the best of your artwork
send it in the correct digital format**

All articles accepted for publication in Elsevier Science journals are processed using electronic production methods. Authors should therefore ensure that their artwork conforms to the following guidelines:

- **Colour and greyscale images** should be supplied as **TIFF** or **EPS** files (resolution 300 dpi).
- **Line drawings (black & white or colour)** should be supplied as **EPS** files

*If you need help to create files in these formats, go to
www.elsevier.com/locate/authorartwork/formats*

Please also note:

- We still need a good quality hard copy of each figure in case the electronic file cannot be used. The hard copy and electronic file must match exactly.
- We can use floppy disks, ZIP disks or CD-ROM. Artwork files should be on a separate disk or CD to article text files.
www.elsevier.com/locate/authorartwork/media
- Only standard fonts should be used, for example: *Times, Times New Roman, Helvetica, Arial, Symbol*
www.elsevier.com/locate/authorartwork/formats
- Lines should be a minimum width of 0.5 pt.
www.elsevier.com/locate/authorartwork/linewidth
- Only standard colours should be used.
www.elsevier.com/locate/authorartwork/colours
- Lettering should be a consistent size and appropriate to the size of the figure.
www.elsevier.com/locate/authorartwork/sizing
- An image which looks acceptable on a computer may not reproduce well, so it is important to ensure that these guidelines are followed.

*Our Author Artwork website has all the information you need on
how to submit your artwork correctly. Visit it today at:*

www.elsevier.com/locate/authorartwork



ELSEVIER



NORTH
HOLLAND



PERGAMON